Journal of Molecular Catalysis B: Enzymatic 70 (2011) 119–126

Contents lists available at ScienceDirect

Journal of Molecular Catalysis B: Enzymatic

journal homepage: www.elsevier.com/locate/molcatb

Immobilization of *Kluyveromyces lactis* β galactosidase on concanavalin A layered aluminium oxide nanoparticles—Its future aspects in biosensor applications

Shakeel Ahmed Ansari, Qayyum Husain*

Department of Biochemistry, Faculty of Life Sciences, Aligarh Muslim University, Aligarh 202002, India

ARTICLE INFO

Article history:
Received 13 December 2010
Received in revised form 20 January 2011
Accepted 23 February 2011
Available online 1 March 2011

Keywords:
Aluminium oxide nanoparticles
Atomic force microscopy
β galactosidase
Concanavalin A
Fourier transform-infrared spectroscopy
Thermogravimetric analysis

ABSTRACT

Several new types of carrier and technology have been implemented in the recent past to improve traditional enzyme immobilization which aims to enhance enzyme loading, activity and stability in order to decrease the cost of enzyme in industrial processes. Thus, the present study aimed to work out a simple and high yield procedure for the immobilization of *Kluyveromyces lactis* β galactosidase on a bioaffinity support, concanavalin A layered Al_2O_3 nanoparticles (Con A layered Al_2O_3-NPs). Thermogravimetric analysis of bioaffinity support revealed 6% loss in weight at 600 °C whereas its thermal decomposition was observed at 350 °C by differential thermal analysis. No significant change was noticed in the band intensity of pUC19 plasmid upon its treatment with Con A layered Al_2O_3-NPs. Comet assay further exhibited negligible change in tail length of comet after treating the lymphocytes by bioaffinity matrix. Atomic force microscopy revealed large surface area of Con A layered Al_2O_3-NPs for binding higher amounts of enzyme. Moreover, Fourier transform-infrared spectroscopy confirmed binding of β galactosidase on bioaffinity support by exhibiting broadening in peaks at 3220.61 cm^{-1} and 3447.27 cm^{-1}. Soluble and immobilized β galactosidase showed same pH-optima at pH 7.0. However, immobilized enzyme exhibited enhanced pH stability and broad spectrum temperature optimum than soluble β galactosidase. Immobilized β galactosidase was found to be highly stable against product inhibition by galactose and retained 85% activity after its sixth repeated use.

1. Introduction

Biotechnology is currently considered as a useful alternative to conventional process technology in industrial and analytical fields. Over last few decades, intense research in enzyme technology has provided many approaches that facilitate their practical applications [1,2]. Among them, new technological development in the field of immobilized biocatalyst offers the possibility of a wider and more economical exploitation of biocatalyst in industry, medicine, waste treatment and in development of bioprocess monitoring devices like biosensors [3–5]. The selected procedure of immobilizing enzyme should be able to stabilize the macromolecules to allow easier diffusion of substrates and products [6,7]. However, only few immobilization methods can control the spatial distribution of catalyst. Therefore, stabilization of enzymes against several physical and chemical denaturants has been accomplished using a multitude of immobilization strategies which include covalent coupling, adsorption, microencapsulation, polymer entrapment and chemical aggregation [8–10].

Procedures which utilize the affinity of biomolecules and ligands for immobilization of enzymes are gaining wider acceptance in constructing sensitive enzyme-based analytical devices as well for other applications. Recently, nanoparticles have emerged as a versatile tool for generating excellent supports for enzyme stabilization due to their small size and large surface area. These molecules influence mechanical properties like stiffness and elasticity thereby reducing diffusion limitations and maximizing the functional surface area to increase enzyme loading [11–13]. Thus, enzymes have been successfully immobilized on nanomaterials by covalent binding, adsorption and entrapment to enhance the performance of enzyme-based biocatalytic sensors [10,14].

Several techniques have been employed previously for immobilization of β galactosidases and these included entrapment [15], crosslinking [16], adsorption [17] and covalent attachment [18]. However, bioaffinity based procedures of enzyme immobilization are attracting much attention due to reversibility, lack of chemical modification and the usually accompanying stability enhancement [19,20]. Moreover, this procedure gives oriented immobilization to

Abbreviations: Con A, concanavalin A; ONPG, *o*-nitrophenyl β-D-galactopyranoside; SβG, soluble β galactosidase; IβG, Con A layered Al_2O_3 nanoparticles adsorbed β galactosidase; DTA, differential thermal analysis; TGA, thermogravimetric analysis; FT-IR, Fourier transform-infrared spectroscopy; AFM, atomic force microscopy.

* Corresponding author. Tel.: +91 571 2700741 (O)/+91 571 2720135 (R); fax: +91 571 2706002; mobile: +91 9808614786.
E-mail addresses: qayyumbiochem@gmail.com, qayyum.husain@amu.ac.in (Q. Husain).

1381-1177/$ – see front matter © 2011 Elsevier B.V. All rights reserved.
doi:10.1016/j.molcatb.2011.02.016

enzymes that facilitated good expression of activity and reusability [21,22]. This method of enzyme immobilization retained very high enzyme activity as no modification/distortion occurs at the active site of enzyme. Since active site is less hindered by nano matrix, the steric accessibility allows more free access for incoming substrate and outgoing products. Moreover, affinity binding offers very mild, controlled adsorption of biocatalysts onto the supports and is likely to be of continuing value for immobilization of sensitive biocatalysts [7,23].

In this study, a novel and efficient method for the immobilization of *Kluyveromyces lactis* β galactosidase on concanavalin A (Con A) layered Al_2O_3 nanoparticles (Al_2O_3-NPs) has been developed. Thermal behavior of bioaffinity support was studied by thermogravimetric analysis (TGA) and differential thermal analysis (DTA). Genotoxicity of the bioaffinity support was checked by pUC19 plasmid nicking assay and comet assay. Immobilized β galactosidase was characterized by atomic force microscopy (AFM) and Fourier transform-infrared (FT-IR) spectroscopy. Effect of pH, temperature and galactose on the activity of soluble and immobilized β galactosidase was monitored. Reusability of immobilized β galactosidase was also evaluated.

2. Materials and methods

2.1. Materials

Al_2O_3-NPs (10 nm) and Lactozym 5000, a liquid preparation of yeast lactase derived from *K. lactis*, were obtained from Sigma Chem. Co. (St. Louis, MO, USA). 2-Nitrophenyl β-D galactopyranoside (ONPG) and concanavalin A (Con A) were obtained from SRL Chemicals (Mumbai, India). All reagents were prepared in double distilled water with chemicals of analytical grade.

2.2. XRD analysis of Al_2O_3 nanoparticles

X-ray diffraction (XRD) pattern of Al_2O_3-NPs was recorded at room temperature using Rigaku Miniflex X-ray diffractometer with Cu Kα radiation ($\lambda = 1.54060$ Å) in 2θ ranging from 20° to 80°. Scherer's formula was used to determine the particle size (D) of the sample: $D = 0.9\lambda/B\cos\theta$, where λ is the X-ray wavelength (1.54060 Å), B is the full width at half-maximum of Al_2O_3 (4 0 0) line and θ is the diffraction angle.

2.3. Preparation of bioaffinity support using Al_2O_3-NPs

Al_2O_3-NPs (100 mg) was added to 1.0 mL of 0.1 M sodium phosphate buffer, pH 7.0 containing Con A (60 mg/mL). The reaction was allowed to proceed overnight at 30 °C with gentle stirring. Con A layered Al_2O_3-NPs were collected by centrifugation at 3000 × *g* for 20 min and were washed thrice with 0.1 M sodium phosphate buffer, pH 7.0. The obtained Con A layered Al_2O_3-NPs were used to immobilize β galactosidase [20].

2.4. Thermogravimetric analysis and differential thermal analysis of Con A layered Al_2O_3-NPs

Thermogravimetric analysis was performed with a Mettler-3000 thermal analyzer using 2 mg sample with heating rate of 10 °C/min in N_2 atmosphere. Differential thermal analysis was also carried out in similar heating range by using TA Instruments Q200 Differential Scanning Calorimeter (DSC).

2.5. Genotoxicity of the bioaffinity support by plasmid nicking assay

Plasmid nicking assay was performed with slight modifications by pUC19 DNA according to the procedure described by Kitts et al. [24]. Reaction mixture (30 μL) containing 10 mM Tris–HCl buffer, pH 7.5, pUC19 DNA plasmid (0.5 μg) and Con A layered Al_2O_3-NPs (10 μL) were incubated for 2 h at 37 °C. Ten microlitres of a solution containing 40 mM EDTA, 0.05% bromophenol blue (tracking dye) and 50% (v/v) glycerol was added after incubation and the solution was then subjected to electrophoresis in submarine 1.0% agarose gel. Ethidium bromide stained gel was then viewed and photographed on a UV-transilluminator.

2.6. Comet assay (single cell gel electrophoresis) of the bioaffinity support

Comet assay was performed with slight modifications according to the procedure described by Dhawan et al. [25]. Fully frosted microscopic slides pre-coated with 1.0% normal melting agarose (PBS buffer lacking Ca^{2+} and Mg^{2+} ions) were used at 50 °C. Cells (10,000) were mixed with 80 μL of 1.0% low melting point agarose to form a cell suspension and were pipetted over the first layer and covered immediately by a cover slip. The slides were placed on a flat tray and kept on ice for 10 min to solidify agarose. Cover slips were removed and 0.5% low melting point agarose (80 μL) was layered which were then allowed to solidify on ice for 5 min. The cover slips were removed and slides were immersed in cold lysis buffer containing 2.5 M NaCl, 100 mM EDTA and 10 mM Tris, pH 10. Triton X-100 (1.0%) was added for 1 h at 4 °C. After lysis, DNA was allowed to unwind for 30 min in alkaline electrophoretic solution consisting of 300 mM NaOH and 1.0 mM EDTA, pH > 13. Electrophoresis was performed at 4 °C in field strength of 0.7 V/cm and 300 mA current. The slides were then neutralized with cold 0.4 M Tris, pH 7.5 stained with 75 mL ethidium bromide (20 mg/mL) and covered with a cover slip. They were then placed in a humidified chamber to prevent drying of gel and analyzed the same day. Slides were scored using an image analysis system (Comet 5.5; Kinetic Imaging, Liverpool, UK) attached to an Olympus fluorescent microscope (CX 41, Olympus Optical Co., Tokyo, Japan) and a COHU 4910-integrated CC camera (equipped with 510–560 nm excitation and 590 nm barrier filters) (COHU, San Diego, CA, USA). Comets were scored at 100× magnification. Images from 50 cells (25 from each replicate slide) were analyzed. The parameter taken to assess lymphocytes DNA damage was tail length in μm (migration of DNA from the nucleus) and was automatically generated by the Comet 5.5 image analysis system.

2.7. Biospecific adsorption of β galactosidase on Con A layered Al_2O_3-NPs

β galactosidase (2520 U) was mixed with Con A layered Al_2O_3-NPs and this mixture was stirred overnight in potassium phosphate buffer, pH 7.0 at 30 °C. The bioaffinity adsorbed β galactosidase was collected by centrifugation at 3000 × *g* for 20 min. Con A layered Al_2O_3-NPs bound β galactosidase was washed thrice with 0.1 M potassium phosphate buffer, pH 7.0 and finally suspended in the same buffer and stored at 4 °C for further use [20].

2.8. Atomic force microscopy (AFM)

Tapping mode AFM experiments of Con A, Al_2O_3-NPs, Con A-Al_2O_3-NPs and Con A-Al_2O_3-NPs adsorbed β galactosidase were performed using commercial etched silicon tips as AFM probes with typical resonance frequency of ca. 300 Hz (RTESP, Veeco).

2.9. FT-IR spectra of Con A, Al_2O_3-NPs, Con A layered Al_2O_3-NPs and Con A layered Al_2O_3-NPs adsorbed β galactosidase

FT-IR spectra of Con A, Al_2O_3-NPs, Con A-Al_2O_3-NPs and Con A-Al_2O_3-NPs adsorbed β galactosidase were monitored with INTERSPEC 2020 model FT-IR instrument, USA. The calibration was done by polystyrene film. The samples were injected by Hamiet 100 μL syringe in ATR box. The syringe was first washed with acetone followed by distilled water. FT-IR analysis was done to monitor functional groups of the compounds.

2.10. Effect of pH and temperature

Enzyme activity of soluble and immobilized β galactosidase (2.5 U) was assayed in the buffers of different pH (4.0–9.0). The buffers were sodium acetate (pH 4.0, 5.0), potassium phosphate (6.0, 7.0) and Tris–HCl (pH 8.0, 9.0). The molarity of each buffer was 0.1 M. The activity at pH 7.0 was taken as control (100%) for the calculation of remaining percent activity.

The activity of soluble and immobilized β galactosidase (2.5 U) was measured at various temperatures (30–70 °C). The enzyme activity at 40 °C was taken as control (100%) for the calculation of remaining percent activity.

2.11. Effect of galactose

The activity of free and immobilized β galactosidase (2.5 U) was determined in the presence of increasing concentrations of galactose (1.0–5.0%, w/v) in 0.1 M potassium phosphate buffer, pH 7.0 at 40 °C for 1 h. The activity of enzyme without added galactose was considered as control (100%) for the calculation of remaining percent activity.

2.12. Reusability of immobilized enzyme

Immobilized β galactosidase (10 U) was taken in triplicates for assaying its activity upon repeated uses. After each assay, immobilized enzyme was washed with 0.1 M potassium phosphate buffer, pH 7.0 by centrifugation at 3000 × *g* for 10 min. The obtained pellet was stored in assay buffer at 4 °C and this process was repeated for seven successive days. The activity determined on first day was considered as control (100%) to calculate remaining percent activity after repeated uses.

2.13. Assay of β galactosidase

The hydrolytic activity of β galactosidase was determined using slight modification in the assay procedure developed by Goddard et al. [26]. The reaction was performed in a total volume of 2.0 mL containing 1.79 mL of 0.1 M potassium phosphate buffer, pH 7.0, 2.5 U β galactosidase and 0.2 mL of 2.0 mM ONPG for 15 min at 40 °C. The reaction was stopped by adding 2.0 mL of 1.0 M sodium carbonate solution and the product formed was measured spectrophotometrically at 405 nm.

One unit (1.0 U) of β galactosidase activity is defined as the amount of enzyme that liberates 1.0 μmole of *o*-nitrophenol (ε_m = 4500 L/mol/cm) per min under standard assay conditions.

2.14. Estimation of protein

Protein concentration was determined by dye binding method [27]. Bovine serum albumin was used as standard protein.

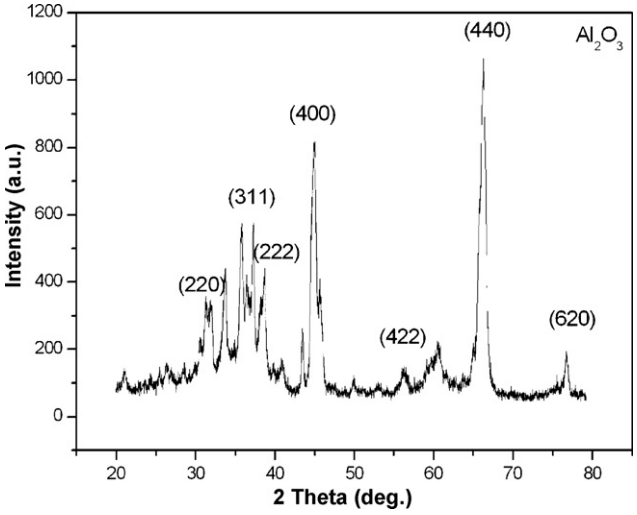

Fig. 1. XRD analysis of Al_2O_3-NPs. X-ray diffraction (XRD) pattern of Al_2O_3-NPs was recorded at room temperature using Rigaku Miniflex X-ray diffractometer with Cu Kα radiation (λ = 1.54060 Å) in 2θ ranging from 20° to 80°. The particle size of the sample was found to be ~10 nm which was estimated from the 4 0 0 line width of XRD peak.

2.15. Statistical analysis

Each value represents the mean for three independent experiments performed in triplicates, with average standard deviations <5%. The data expressed in various studies was plotted using Sigma Plot-9. Data was analyzed by one-way ANOVA. *P*-values <0.05 were considered statistically significant.

3. Results

3.1. XRD analysis of Al_2O_3-NPs

XRD pattern of Al_2O_3-NPs showed that the sample was in cubic crystal symmetry and exhibited face centered lattice (Fig. 1). The lattice parameter calculated from XRD pattern was *a* = 7.941. The observed 2θ values were consistent with the standard Joint Committee on Powder Diffraction Standards (JCPDS) value (file no 79-1558). The particle size analyzed from 400 line width of XRD peaks of the sample was found to be ~10 nm.

3.2. TGA and DTA of Con A layered Al_2O_3-NPs

TGA curve of the bioaffinity matrix exhibited 6% weight loss at 600 °C while the DTA curve revealed the beginning of its thermal decomposition at 350 °C (Fig. 2).

3.3. Treatment of pUC19 DNA with Con A layered Al_2O_3-NPs

The damaging effect of a bioaffinity support on plasmid DNA was negligible as the band intensity of treated sample was similar to that of control (Fig. 3a). Since the nicking of plasmid was not affected by DNA fragmentation assays, thus Con A layered Al_2O_3-NPs was exploited to immobilize β galactosidase.

3.4. Effect of bioaffinity support, Con A layered Al_2O_3-NPs on DNA breakage in lymphocyte

Fig. 3b (i) shows that Con A layered Al_2O_3-NPs exhibited only a minor degree of nuclear DNA breakage which was shown by histogram in terms of the tail length of comet as an indicator of percent DNA damage Fig. 3b (ii).

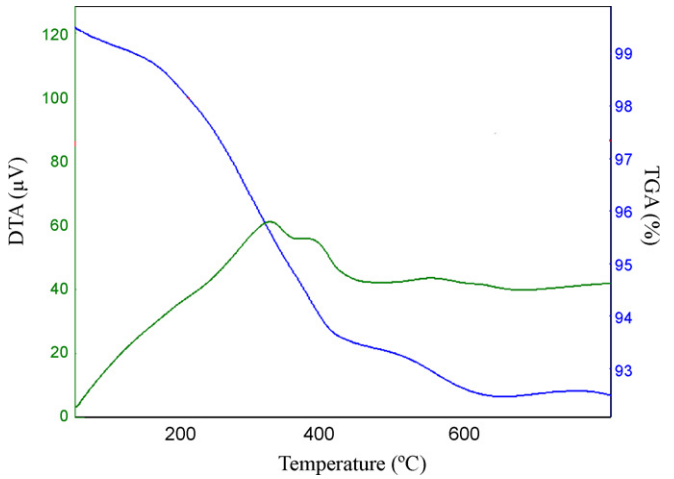

Fig. 2. TGA and DTA of Con A layered Al_2O_3-NPs. Thermogravimetric analysis was performed with a Mettler 3000 thermal analyzer using 2 mg sample with heating rate of 10 °C/min in N_2 atmosphere. Differential thermal analysis was also carried out in similar heating range by using TA Instruments Q200 Differential Scanning Calorimeter (DSC).

3.5. Immobilization of β galactosidase on Con A layered Al_2O_3-NPs

Table 1 demonstrates the immobilization of β galactosidase on Con A layered Al_2O_3-NPs, a bioaffinity support. Con A layered Al_2O_3-NPs adsorbed 93% of the original enzyme activity.

3.6. AFM measurement

AFM image of Con A layered Al_2O_3-NPs revealed a smoother surface over long length scales forming a well established matrix for the immobilization of β galactosidase (Fig. 4).

3.7. FT-IR analysis

Fig. 5 shows FT-IR spectra of Al_2O_3-NPs and its complex with Con A and finally the binding of β galactosidase with Con A-Al_2O_3-NPs. FT-IR analysis of Con A revealed the presence of amide I (1649.91 cm^{-1}), amide II (1542.54 cm^{-1}), amide III (1232.38 cm^{-1}) and amide IV (671.70 cm^{-1}) bands. The stretching of carbonyl group of β galactosidase was observed by broadening of peaks at 3220.61 cm^{-1} and 3447.27 cm^{-1}.

3.8. Effect of pH and temperature

pH–activity profiles for soluble and immobilized β galactosidase are shown in Fig. 6. Both soluble and immobilized enzyme exhibited same pH-optima at pH 7.0. Soluble enzyme showed 52% activity at pH 6.0 while the immobilized enzyme retained 78% activity under identical experimental conditions.

Fig. 7 demonstrates temperature–activity profiles for soluble and immobilized enzyme. Immobilized β galactosidase exhibited broadening in temperature-optimum from 40 °C to 50 °C. Con A layered Al_2O_3-NPs adsorbed β galactosidase retained 86% catalytic activity at 60 °C while the free enzyme exhibited only 27% at this temperature.

3.9. Effect of galactose

Galactose is one of the end products of β galactosidase catalyzed hydrolysis of lactose. The activity of soluble and immobilized β galactosidase was investigated in the presence of various concentrations (1.0–5.0%, w/v) of galactose (Fig. 8). Incubation of soluble β galactosidase with 3.0% galactose for 1 h at 37 °C resulted in a loss of 51% of the initial activity while immobilized enzyme retained over 68% activity under similar incubation conditions.

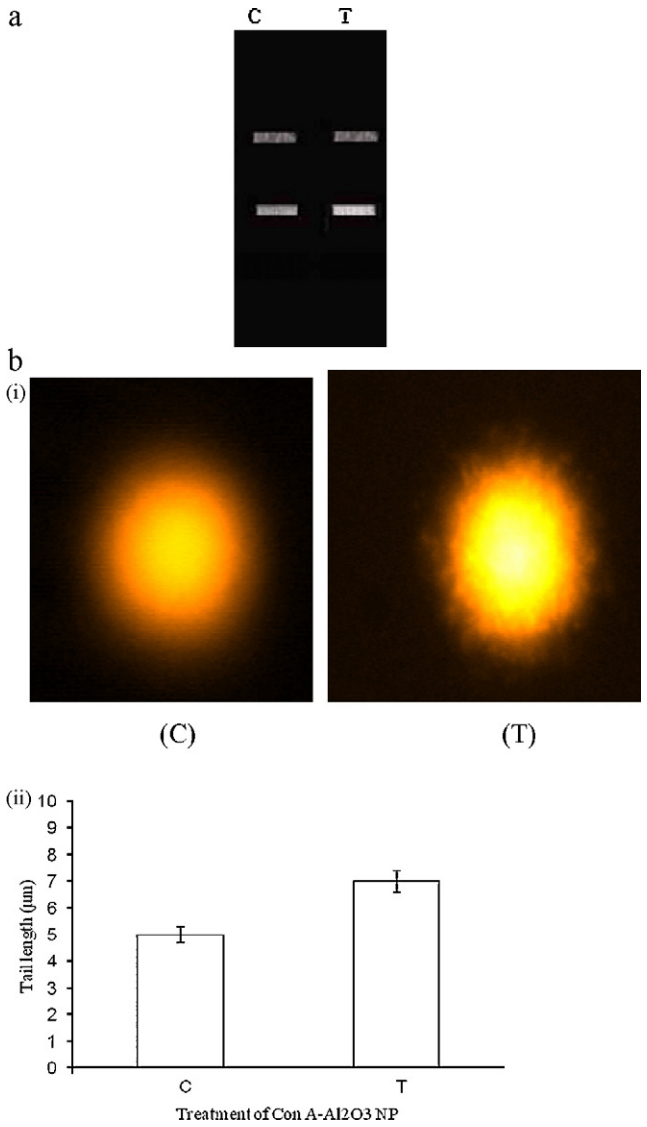

Fig. 3. (a) Plasmid nicking toxicity assay for Con A layered Al_2O_3-NPs. Toxicity of the bioaffinity support was analyzed by plasmid nicking assay as given in the text. Circular double stranded pUC19 DNA was used. Lane (C) denotes control pUC19 DNA while lane (T) signify pUC19 DNA incubated with Con A layered Al_2O_3-NPs. (b) (i): Comet assay for Con A layered Al_2O_3-NPs. Quantitative analysis of nuclear DNA damage was observed by Comet assay as given in the text. The microscopic images of control DNA (C) and DNA treated with Con A layered Al_2O_3-NPs (T) have been shown. (b) (ii): Comet assay for Con A layered Al_2O_3-NPs. A histogram showing control (C) and Con A layered Al_2O_3-NPs induced DNA breakage in lymphocyte (T).

3.10. Reusability of immobilized enzyme

Reusability is one of the significant indices to evaluate the property of immobilized enzyme at large scale. Fig. 9 shows the residual activity of immobilized enzyme upon subsequent uses. Immobilized β galactosidase retained 91% of the initial activity after its fourth repeated use.

Table 1
β galactosidase immobilized on Con A layered Al_2O_3-NPs.

Enzyme activity loaded, X (U)	Enzyme activity in washes, Y (U)	Activity bound/100 mg Con A-Al_2O_3-NPs		Activity yield (%) $B/A \times 100$
		Theoretical $(X-Y)=A$	Actual $=B$	
2520	363	2157	2006	93

Each value represents the mean for three independent experiments performed in triplicates, with average standard deviations, <5%.

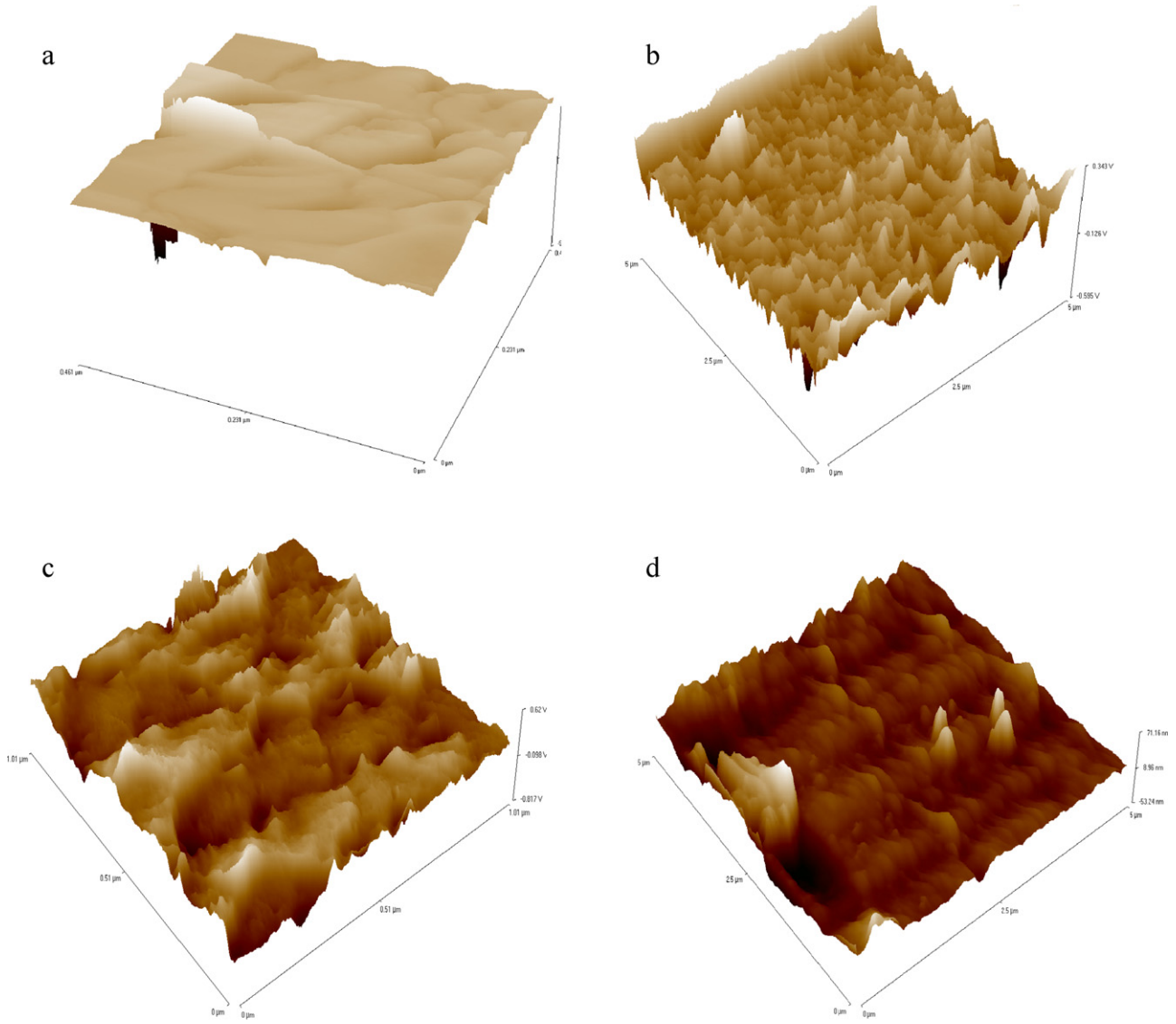

Fig. 4. Atomic force microscopy of Con A, Al_2O_3-NPs, Con A layered Al_2O_3-NPs and Con A layered Al_2O_3-NPs adsorbed β galactosidase. Tapping mode AFM experiments were performed using commercial etched silicon tips as AFM probes with typical resonance frequency of 300 Hz (RTESP, Veeco). Atomic force micrographs for (a) Con A, (b) Al_2O_3-NPs, (c) Con A layered Al_2O_3-NPs and (d) Con A layered Al_2O_3-NPs adsorbed β galactosidase have been shown.

4. Discussion

Nanoparticles based enzyme immobilization is an enigma that deserves special attention as it provides greater surface area for binding higher amount of enzyme to matrix, prevents unfolding of protein and permits greater flexibility for conformational changes required for enzyme activity [12,28]. Other advantages involved with their use include continuous operations, catalyst recycling, enhanced stability, easy separation from reaction mixture, possible modulation of the catalytic properties and much easier prevention of microbial growth [18,29].

In the recent past, Al_2O_3-NPs has been exploited as a potential candidate in targeted drug delivery and biosensor application [30,31] but no study has been carried out which could strengthen its importance in immobilizing industrially important enzymes. Thus, in the present manuscript, a high yield immobilized preparation was obtained by specific adsorption of *K. lactis* β galactosidase on a highly efficient and selective bioaffinity support, Con A layered Al_2O_3-NPs (Table 1).

XRD analysis showed cubic crystal symmetry and face centered lattice of Al_2O_3-NPs. The lattice parameters calculated from the XRD pattern were $a=7.941$. The observed 2θ values were consistent with the standard JCPDF value (file no 79-1558). The particle

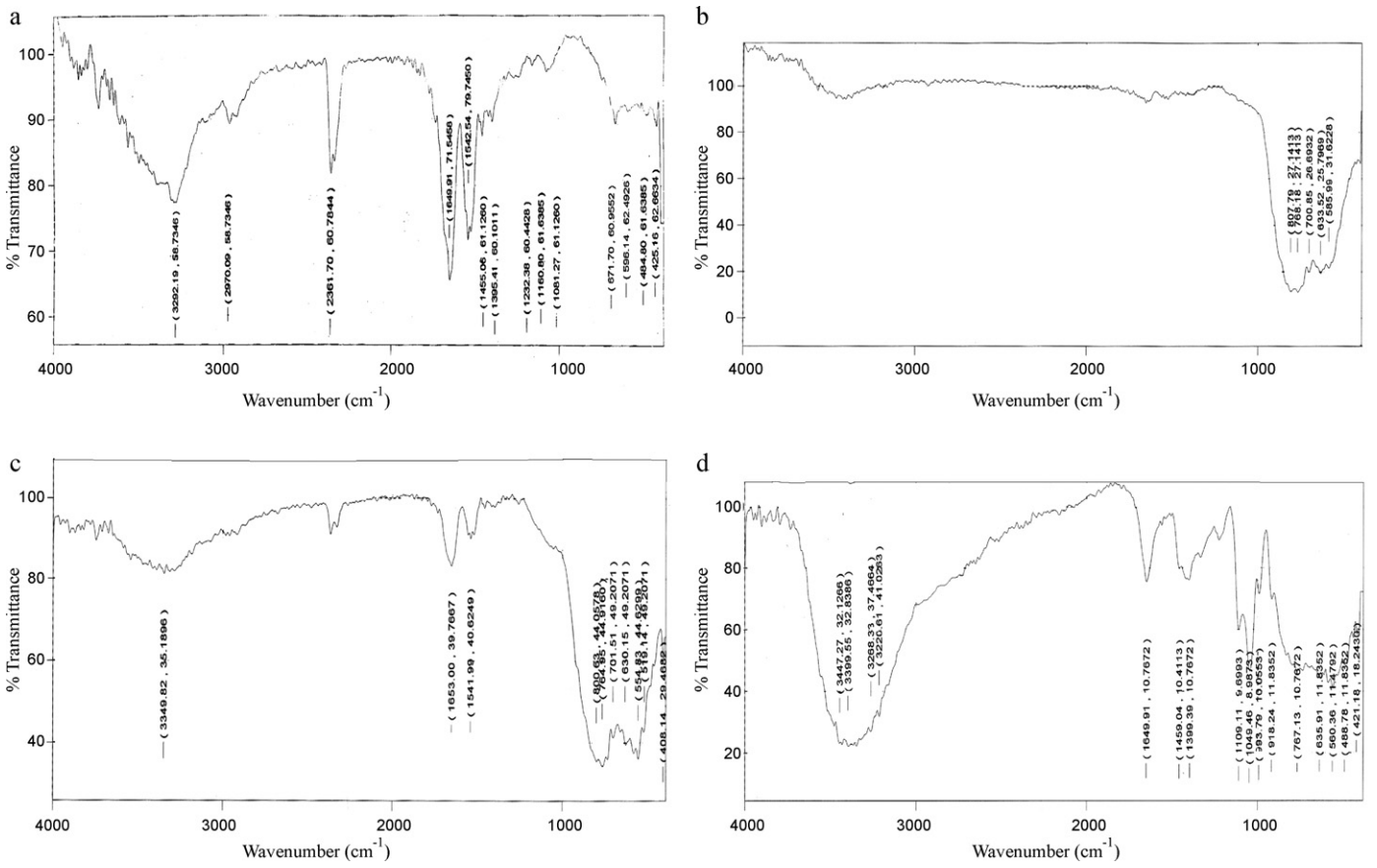

Fig. 5. FT-IR spectra of Con A, Al_2O_3-NPs, Con A layered Al_2O_3-NPs and Con A layered Al_2O_3-NPs adsorbed β galactosidase. FT-IR analysis was done to monitor the linkages between Con A layered Al_2O_3-NPs and β galactosidase. FT-IR spectra of (a) Con A, (b) Al_2O_3-NPs, (c) Con A layered Al_2O_3-NPs and (d) and Con A layered Al_2O_3-NPs adsorbed β galactosidase were monitored with INTERSPEC 2020 model FT-IR instrument, USA. The calibration was done by polystyrene film. The syringe was first washed with acetone followed by distilled water. The samples were injected by Hamiet 100 μL syringe in ATR box.

size estimated from the 400 line width of the XRD peaks of sample was found to be ~10 nm (Fig. 1).

It was essential to demonstrate the genotoxic effect of Con A layered Al_2O_3-NPs on pUC19 DNA plasmid (which was observed by DNA fragmentation assay) so that it could be exploited in biosensor application and in novel targeted drug delivery for lactose intolerant patients. It was observed that the bioaffinity support did not induce breakage in pUC19 DNA, thereby indicating non-toxicity of the bioaffinity support (Fig. 3a). Single-cell gel electrophoresis (SCGE) is a very sensitive method for measuring DNA strand breaks in individual cells. It is widely used in environmental toxicology, cancer research and radiation biology to assess DNA damage. Damaged DNA migrates during electrophoresis from nucleus towards anode, forming a shape of a "comet" with a head (cell nucleus with intact DNA) and a tail (relaxed and broken DNA). Here, comet showed slightly broadened appearance thereby indicating no damage to DNA (Fig. 3b (i)) which was further shown by only 2 μm damage to DNA in the histogram (Fig. 3b (ii)). Such findings have never been reported for any immobilized β galactosidase system. Due to easy production, excellent temperature stability, non-toxic

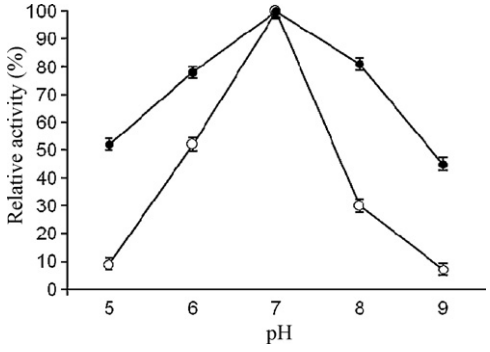

Fig. 6. pH activity profiles for soluble and immobilized β galactosidase. The activity of soluble and immobilized β galactosidase (2.5 U) was measured at 40 °C in the buffers of various pHs (3.0–9.0). The buffers used were sodium acetate (pH 4.0, 5.0), potassium phosphate (6.0, 7.0) and Tris–HCl (pH 8.0, 9.0). Molarity of each buffer was 0.1 M. Activity at pH 7.0 was taken as control (100%) for the calculation of remaining percent activity. Symbols show (○) soluble and (●) immobilized β galactosidase.

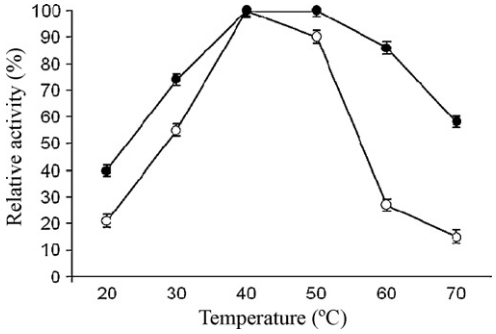

Fig. 7. Temperature activity profiles for soluble and immobilized β galactosidase. The activity of soluble and immobilized β galactosidase (2.5 U) was assayed in 0.1 M potassium phosphate buffer, pH 7.0 at various temperatures (30–70 °C) for 15 min. Activity obtained at 40 °C was considered as control (100%) for the calculation of remaining percent activity. For symbols, please refer to Fig. 6.

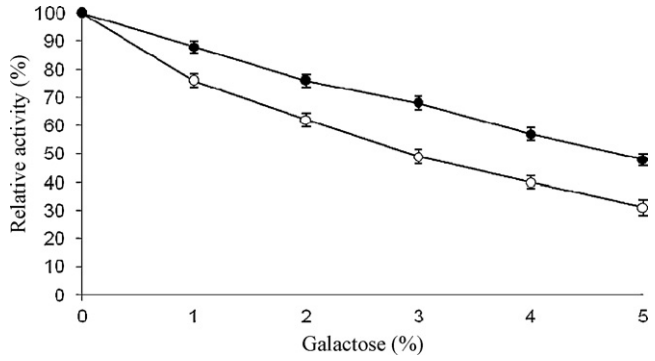

Fig. 8. Effect of galactose on soluble and immobilized β galactosidase (2.5 U) was measured in the presence of increasing concentrations of galactose (1.0-5.0%, w/v) in 0.1 M potassium phosphate buffer, pH 7.0 for 1 h at 40 °C. Activity of enzyme without added galactose was considered as control (100%) for the calculation of remaining percent activity at other concentrations. For symbols, please refer to Fig. 6.

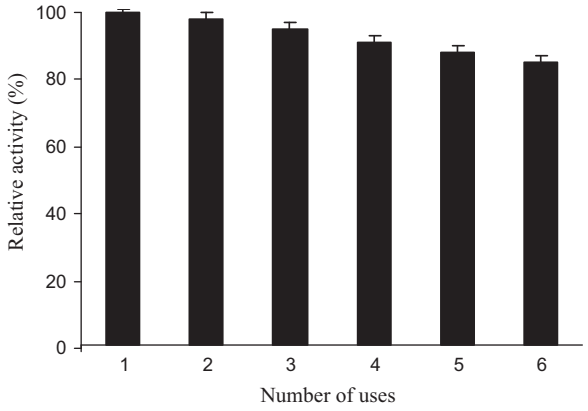

Fig. 9. The reusability of immobilized β galactosidase was monitored for six successive days. The preparation was taken in triplicates and was assayed for remaining percent activity. Activity determined on first day was taken as control (100%) for the calculation of remaining activity after each use.

nature and greater specificity of the bioaffinity support, it might serve as a powerful biorecognition probe in biosensor applications.

It is well documented that properties and performance of broad range of materials depends on their surface characteristics. Atomic force micrographs of Con A revealed that it provided large surface area for enzyme immobilization (Fig. 4a). Al_2O_3-NPs appeared heterogeneous in terms of particle size and shape besides representing smooth surface over long length scales (Fig. 4b). Moreover, Fig. 4c revealed that Con A layered Al_2O_3-NPs exhibited uniform monolayer over long distances and form a well-established matrix for the immobilization of β galactosidase.

FT-IR analysis of Con A revealed the presence of amide I (1649.91 cm^{-1}), amide II (1542.54 cm^{-1}), amide III (1232.38 cm^{-1}) and amide IV (671.70 cm^{-1}) bands (Fig. 5a). It manifested that its main structure comprised α and β helix with greater predominance of β sheeted structures [32]. The peaks stretched between 585.99 cm^{-1} and 807.79 cm^{-1} confirmed Al_2O_3-NPs peaks (Fig. 5b). The peaks observed at 1541.99 cm^{-1} and 1653 cm^{-1} signify binding of Con A on Al_2O_3-NPs (Fig. 5c). Moreover, the peak of water present in medium was noticed at 3349.82 cm^{-1} [33,34]. Furthermore, the stretching of carbonyl group of β galactosidase was observed by broadening of peaks from 3220.61 cm^{-1} and 3447.27 cm^{-1} which showed its adsorption on Con A layered Al_2O_3-NPs (Fig. 5d). Similar broadening of peaks was obtained between 421.18 cm^{-1} and 767.13 cm^{-1} for Al_2O_3-NPs while new peaks observed at 1049.46 cm^{-1} and 1109.11 cm^{-1} denote attachment of Al_2O_3-NPs with –OH group of β galactosidase [35].

The stability against various denaturing agents is an important factor when selecting an appropriate enzymatic system for any application. The generally observed higher stability of bioaffinity bound β galactosidase against various forms of inactivation may be related to specific and strong binding of enzyme with bioaffinity support which prevented its unfolding/denaturation [7,36]. Enhanced pH stability and broad spectrum temperature stability of immobilized enzyme reflected its antithermal property which might be attributed to conformational stability attained by enzyme as a result of bond formation between enzyme and matrix or lower restriction to substrate diffusion at higher temperatures (Figs. 6 and 7). Immobilized β galactosidase showed greater resistance to product inhibition mediated by galactose (Fig. 8) as compared to *Aspergillus oryzae* β galactosidase immobilized on Con A-cellulose [20].

High costs of enzymes used for industrial purposes and the time necessary for their immobilization for subsequent use have led to increase the possibility of reusing immobilized enzyme [3,37]. Con A layered Al_2O_3-NPs adsorbed β galactosidase retained nearly 85% activity after its sixth repeated use (Fig. 9), thus it provides a cost effective advantage for its exploitation in an economically viable enzyme catalyzed process.

5. Conclusion

The selection of Al_2O_3-NPs for β galactosidase immobilization revealed a stable and non-toxic enzyme-matrix interaction. This type of novel bioaffinity support could serve as a potential enzyme immobilization carrier for several industrial applications. Such immobilized enzyme preparation can be utilized in hydrolyzing lactose from milk and whey in continuous stirred tank bioreactors. Utility of the method can be further extended in development of therapeutic agents as novel targeted drug delivery for lactose intolerant patients across the globe. Due to easy production, excellent temperature stability, non-toxic nature and greater specificity of bioaffinity support, it might serve as a powerful biorecognition probe in biosensor applications.

Acknowledgements

Council of Science and Technology, Uttar Pradesh, India is gratefully acknowledged for funding the project entitled "Immobilization of plant and fungal β galactosidases by using bioaffinity supports—Its application in the hydrolysis of lactose in whey and milk." Mohd Arshad (Department of Chemistry, Jamia Milia Islamia, New Delhi, India) is gratefully acknowledged for the measurement and interpretation of TGA and DTA.

References

[1] N.M. Ravindra, C. Prodan, S. Fnu, I. Padron, S.K. Sikha, J. Miner. Metal. Mater. Soc. 12 (2007) 37–43.
[2] S. Akella, C.K. Mitra, Ind. J. Biochem. Biophys. 44 (2007) 82–87.
[3] E. Logoglu, S. Sungur, Y. Yildiz, J. Macromol. Sci. Part A: Pure Appl. Chem. 43 (2006) 525–533.
[4] R.S. Gaster, D.A. Hall, C.H. Nielsen, S.J. Osterfeld, Nat. Med. 15 (2009) 1327–1332.
[5] Z. Peng, Y. Bin-Cheng, Y. Bang-Ce, Biosens. Bioelectron. 25 (2009) 935–939.
[6] D.A.R. Mahmoud, W.A. Helmy, J. Appl. Sci. Res. 5 (2009) 2466–2476.
[7] Q. Husain, Crit. Rev. Biotechnol. 30 (2010) 41–62.
[8] V. Iyer, L. Ananthanarayan, Proc. Biochem. 43 (2008) 1019–1032.
[9] C. Mateo, J.M. Palomo, G. Fernandez-Lorente, J.M. Guisan, Enzyme Microb. Technol. 40 (2007) 1451–1463.
[10] M. Di Marco, S. Shamsuddin, K.A. Razak, A.A. Aziz, Int. J. Nanomed. 5 (2010) 37–49.
[11] J. Kim, J.W. Grate, P. Wang, Chem. Eng. Sci. 61 (2006) 1017–1026.
[12] R.E. Hamlin, T.L. Dayton, L.E. Johnson, M.S. Johal, Langmuir 23 (2007) 4432–4437.
[13] T. Xie, A. Wang, L. Huang, H. Li, Afr. J. Biotechnol. 8 (2009) 4724–4733.
[14] J. Li, J. Wang, V.G. Gavalas, D.A. Atwood, Nanoletters 3 (2003) 55–58.
[15] L. Betancor, R.H. Luckarift Seo, O. Brand, Biotechnol. Bioeng. 99 (2008) 261–267.

[16] S. Zhang, S. Gao, G. Gao, Appl. Biochem. Biotechnol. 160 (2010) 1386–1393.
[17] S. Gurdas, H.A. Gulec, M. Mutlu, Food Bioprocess. Technol. (2010), doi:10.1007/s11947-010-0384-7.
[18] C. Pan, B. Hu, W. Li, Y. Sun, J. Mol. Catal. B: Enzym. 61 (2009) 208–215.
[19] B. Bucur, A.F. Danet, J.L. Marty, Anal. Chim. Acta 530 (2005) 1–6.
[20] S.A. Ansari, Q. Husain, J. Mol. Catal. B: Enzym. 6 (2010) 68–74.
[21] S. Akhtar, A.A. Khan, Q. Husain, J. Chem. Technol. Biotechnol. 80 (2005) 198–205.
[22] M. Sardar, M.N. Gupta, Enzyme Microb. Technol. 37 (2005) 355–359.
[23] J.L. Ellis, D.L. Tomasko, F. Dehghani, Biomacromolecules 9 (2008) 1027–1034.
[24] D.D. Kitts, A.N. Wijewickreme, C. Hu, Mol. Cell. Biochem. 203 (2000) 1–10.
[25] A. Dhawan, M. Bajpayee, D. Parmar, Cell Biol. Toxicol. 25 (2008) 5–32.
[26] J.M. Goddard, J.N. Talbert, J.H. Hotchkiss, J. Food Sci. 72 (2007) E36–E41.
[27] M.M. Bradford, Anal. Biochem. 72 (1976) 248–255.
[28] D. Cui, H. Gao, Biotechnol. Prog. 19 (2003) 683–692.
[29] D.F.M. Neri, V.M. Balcao, M.G. Carneiro-da-Cunha, L.B. Carvalino Jr., Catal. Commun. 9 (2008) 2334–2339.
[30] A. Frey, M.R. Neutra, F.A. Robey, Bioconjugate Chem. 8 (1997) 424–433.
[31] A. Heilmann, N. Teuscher, A. Kiesow, D. Janasek, J. Nanosci, Nanotechnology 3 (2003) 375–379.
[32] S. Yaowalak, S. Wilaiwan, S. Prasong, J. Appl. Sci. 9 (2009) 2992–2995.
[33] X. Xiang, X.T. Zu, Z.G. Wang, B. Jiang, Mat. Res. Soc. Symp. Proc. 792 (2004), R3.12.1–R3.12.6.
[34] C. Pathmamanoharan, P. Wijkens, D.M. Grove, A.P. Philipse, Langmuir 12 (1996) 4372–4377.
[35] K.M. Naskar, J. Am. Ceram. Soc. 93 (2010) 1260–1263.
[36] Y. Numanoglu, S. Sungur, Process Biochem. 39 (2004) 703–709.
[37] S.K. Sharma, R. Singhal, B.D. Malhotra, N. Sehgal, Biosens. Bioelectron. 20 (2004) 651–657.